Applied Physics B (2020) 126:30
https://doi.org/10.1007/s00340-020-7381-y

Applied Physics B
Lasers and Optics

Investigations of mode-locked Er-doped oscillators with record high-pulse energies

Rui Zhao[1] · Mengxiao Wang[1] · Yue Zheng[1] · Xiaohan Chen[2] · Huanian Zhang[3] · Dengwang Li[1]

Received: 3 October 2019 / Accepted: 13 January 2020 / Published online: 28 January 2020

Abstract
In our experiment, based on nonlinear polarization rotation (NPR), first, we demonstrate a large-energy square-wave mode-locked fiber laser under low pump power. The largest pulse energy of the square-wave pulses was 106.91 nJ. However, pulse breaking occurred when the pump power was higher than 1152 mW. Thus, under the maximum pump power of 2318 mW, several kinds of large-energy mode-locked operations were also investigated successfully. The maximum output pulse energy was recorded to be 881.34 nJ, which exhibits obvious enhancement in comparison with previous works. Additionally, in our work, we have successfully revealed that broadening of the pulse width, splitting of the pulse shape and increasing of the pulse repetition rate play significant roles in reducing the influence of large pulse energy and high peak power experimentally. Our experiment result will provide a useful guide for demonstrating large-energy pulse operations.

1 Introduction

Passively mode-locked fiber lasers have been investigated widely due to their competitive properties including compact structure, low cost, ultrafast pulse width, large pulse energy, high peak power and so on [1–6]. Especially, large-energy mode-locked fiber lasers exhibit various special potential applications in the fields of laser micro-machining, all-optical square-wave clocks, optical sensors, laser ablation, etc. [7–11]. For obtaining high-energy mode-locked pulses, different types of mode-locked fiber lasers including square-wave [12], stretched-pulse [13], self-similar [14, 15], and noise-like and so on [16] have been investigated successfully.

In general, a long-length laser cavity or a high-power pump source will be beneficial for leading to the formation of large-energy pulse operation. In details, Kobtsev et al. designed a ~ 3.8 km length ring Yb-doped laser cavity for producing 3.9 μJ pulse energy with a pulse duration of 3 ns under a repetition rate of 77 kHz [17]. A long-cavity square-wave Er-doped passively mode-locked fiber laser with a pulse energy of 41.8 nJ was reported by Zhang et al. in 2012 [18]. By employing high-power pump source and a long-length laser cavity, simultaneously, stable mode-locked pulses at a repetition rate of 278 kHz with single-pulse energy as high as 715 nJ are obtained by Li et al. [19]. A compact all-fiber high-energy fiber laser consisting of a laser oscillator and a compression section with 8 nJ pulse energy and 290 fs pulse duration was reported in 2010 [20]. Chunmei et al. experimentally demonstrated an all-fiber erbium-doped fiber laser operating in the large normal dispersion regime, which exhibited a pulse duration of 30.5 ps and a pulse energy of 12 nJ [21]. Mao et al. have obtained high-energy rectangular pulses delivering from an erbium-doped fiber laser operating in ultra-large net negative-dispersion regime. The outputted pulses can be amplified to over 2 μJ by a two-stage erbium-doped fiber amplifier [22]. Nikolai et al. generated 20 nJ pulse energy from an Er-doped fiber oscillator, the chirped output pulses with a duration of 53 ps could be compressed to 750 fs [23]. Kai et al. also experimentally demonstrated pulse energy enhancement in a large normal dispersion

✉ Huanian Zhang
huanian_zhang@163.com

✉ Dengwang Li
dengwang@sdnu.edu.cn

[1] Shandong Province Key Laboratory of Medical Physics and Image Processing Technology, School of Physics and Electronics, Shandong Normal University, Jinan 250014, China

[2] Shandong Provincial Key Laboratory of Laser Technology and Application, School of Information Science and Engineering, Shandong University, Jinan 250014, China

[3] School of Physics and Optoelectronic Engineering, Shandong University of Technology, Zibo 255049, China

regime, highly chirped dissipative solitons with pulse energies up to 9.4 nJ were obtained, the fundamental repetition rate was 2.3 MHz, and the pulse duration was 35 ps [24]. Besides the mentioned works which mainly designed based on the NPR technique, generation of mode-locked rectangular pulses with a pulse energy of 3.25 nJ operating in dissipative soliton resonance region is also demonstrated in an erbium-doped figure-eight fiber laser with net anomalous dispersion [25]. Double clad Er/Yb co-doped fiber lasers also have been reported for obtaining large-energy mode-locked operations. F. Sanchez et al. have done several excellent works focusing on the generation of large-energy mode-locked operations based on the double clad Er/Yb co-doped fiber lasers [26–28]. Thereinto, a dual amplifier passive mode-locked figure-of-eight fiber laser system generating 10 μJ tunable dissipative soliton resonance square pulses was reported. In their work, the width of the output laser can be tuned in a range of almost 360 ns [26]. Optimization of the experimental parameters such as the net cavity dispersion, the coupling ratio between the two loops of the cavity and the exact position of the long fiber coils has been identified for obtaining square pulses with an energy varying between 8.5 and 10.1 μJ, while the pulse width ranges from 84 to 416 ns [27]. In addition, emission of an all-fiber laser configuration with a maximum average pulse energy of 1.83 μJ was also investigated under several different values of large anomalous dispersion [29]. It is obvious that based on double clad Er/Yb co-doped fiber lasers, μJ-level pulse energies can be obtained, which show obvious enhancement, however, double clad Er/Yb co-doped fiber lasers also suffer from the effect of high cost. Besides, large-energy mode-locked operations based on real saturable absorbers (SAs) have also been reported successfully. Based on a semiconductor saturable absorber mirror, Tian et al. demonstrated an all-normal-dispersion Yb-doped fiber laser generating 4.3 nJ pulse energy under a repetition rate of 397 kHz [30]. Xu et al. obtained different large-energy mode-locked operations within a Bi_2Se_3-based Er-doped fiber laser. The maximum pulse energy of 17.2 nJ and a pulse width of 187 ns under a pulse repetition rate of 537.6 kHz were obtained [31].

In our experiment, based on the NPR technique with a long-length laser cavity and high-power pump sources, Er-doped mode-locked oscillators with enhanced output pulse energies have been demonstrated successfully. Among which, the largest pulse energy was as high as 881.34 nJ, to our knowledge, which is the recorded pulse energy obtained within Er-doped mode-locked oscillators. Additionally, during the experiment, phenomena including broadening of the pulse width, splitting of the pulse shape and increasing of the pulse repetition rate have been investigated for reducing the influence of the high peak power and large energy under high pump powers.

2 Experimental setup

Figure 1 shows the experimental schematic of the NPR-based passively mode-locked Er-doped fiber laser. As shown, a ring laser cavity including a piece of ~ 61-cm-long Er-doped fiber (EDF) (Er-80, Liekki) with a group velocity dispersion (GVD) of − 20 ps^2/km, ~ 1215 m long single-mode fiber (SMF-28) with a GVD of − 21.68 ps^2/km, two wavelength division multiplexers (WDMs) (WDM1 and WDM2), two PCs (PC1 and PC2), a polarization-dependent isolator (PD-ISO) and a 20/80 optical coupler (OC) is demonstrated. The total length of cavity is 1225 m. Thus, the total net cavity dispersion was calculated to be − 26.6 ps^2. Two 976 nm single-mode laser diodes with a maximum average output power of 1.3 W are employed as pump sources, which were delivered into the laser cavity through WDMs. The PCs and PD-ISO are used for the adjustment of the polarization state and guaranteeing unidirectional propagation of light within the ring laser cavity. The generated fiber laser is delivered out of the cavity through the 80% port of the OC. The output characteristics were recorded by an optical spectrum analyzer (AQ6317B, Yokogawa), an InGaAs photo-detector (PD-03), a digital oscilloscope (Wavesurfer 3054), a frequency spectrum analyzer (R&S FPC1000) and a power meter.

3 Experimental results and discussion

Under the maximum displayed pump power of 2659 mW, the real output power of WDM 1 and 2 was 1108 and 1210 mW, respectively, corresponding to an optical conversion efficiency of 87.18%. The pump power in this paper was calculated by multiplying displayed pump power by the optical conversion efficiency. As mentioned for boosting the pulse energy of the mode-locked laser, based on the NPR technique, a long stretch of single-mode fiber is added into the laser cavity. Meanwhile, a long stretch of fiber without

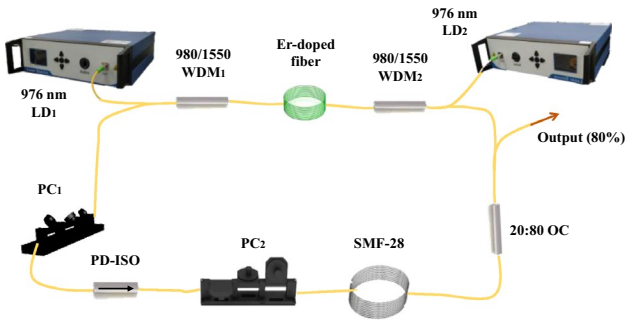

Fig. 1 Schematic of a passively mode-locked high-energy fiber laser

polarization maintenance also leads to the effect of nonlinear polarization evolution, which will acts as an additional mode-locking mechanism. Additionally, long-length single-mode fiber will also lead to a large dispersion value, which exhibits significance in guaranteeing the formations of various solitons. In the experiment, only by adjusting the state of the PCs and the value of the pump power, different kinds of mode-locked operations with large pulse energies were recorded. The characteristics of the mode-locked operations were investigated in detail and described as below.

First, when the pump power ranged from 251 to 974 mW, square-wave mode-locked operation was achieved by rotating the two PCs properly. Figure 2 shows the information of the mode-locked operation under the maximum pump power of 974 mW. The emission spectrum with a central wavelength of 1561.335 nm and a 3 dB bandwidth of ~ 5.847 nm is shown in Fig. 2a. The recorded pulse train is depicted in Fig. 2b, the pulse-to-pulse time is 5.97 μs, corresponding to a cavity length-dependent fundamental pulse frequency of 167.62 kHz. Typical single pulse with a square shape and a pulse width of 81.41 ns is shown in Fig. 2c. The relationship between the pump power and the maximum average output power is described in Fig. 2d, the maximum average output power is as high as 17.92 mW, corresponding to a pulse energy of 106.91 nJ. The long cavity and the insert loss of the intra-cavity components contributed to the low optical conversion efficiency. Radiofrequency (RF) spectra were recorded for testing the stability of the mode-locked operations, Fig. 2e shows the RF spectrum recorded within 250 kHz bandwidth under a resolution of 1 kHz. Obviously, the peak of the fundamental frequency is located at 167.62 kHz with a signal-to-noise ratio of ~ 40 dB. RF spectrum within a 10 MHz bandwidth is also recorded and depicted in Fig. 2f. The wideband RF spectrum also exhibit high signal-to-noise ratios. Therefore, the RF characteristics indicate that mode-locked pulses with high stability are obtained in our work.

Emission spectra under different pump powers were also recorded for better understanding the evolution of the spectra. As is shown in Fig. 3a, the central wavelengths under the pump power of 251 mW, 434 mW, 615 mW, 795 mW and 974 mW are 1559.372 nm, 1559.664 nm, 1561.462 nm, 1560.961 nm and 1561.335 nm, respectively. Meanwhile, the corresponding 3 dB bandwidths are 4.139 nm, 5.090 nm, 6.083 nm, 5.718 nm and 5.847 nm, respectively. However, in the experiment, when the pump power was higher than

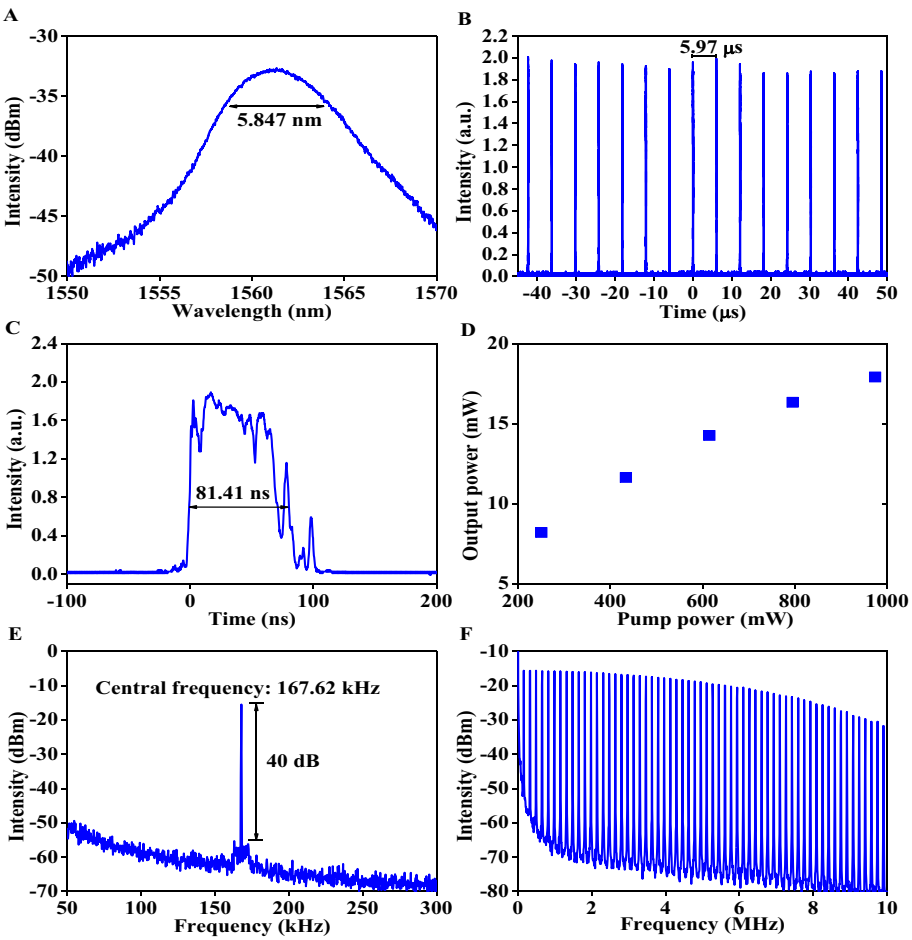

Fig. 2 The output characteristics of the square-wave pulse mode-locked operation under the pump power of 974 mW. **a** Optical spectrum. **b** Pulse train. **c** single-pulse shape. **d** The relationship between output power and pump power. **e** RF spectrum within 250 kHz bandwidth. **f** RF spectrum within 10 MHz bandwidth

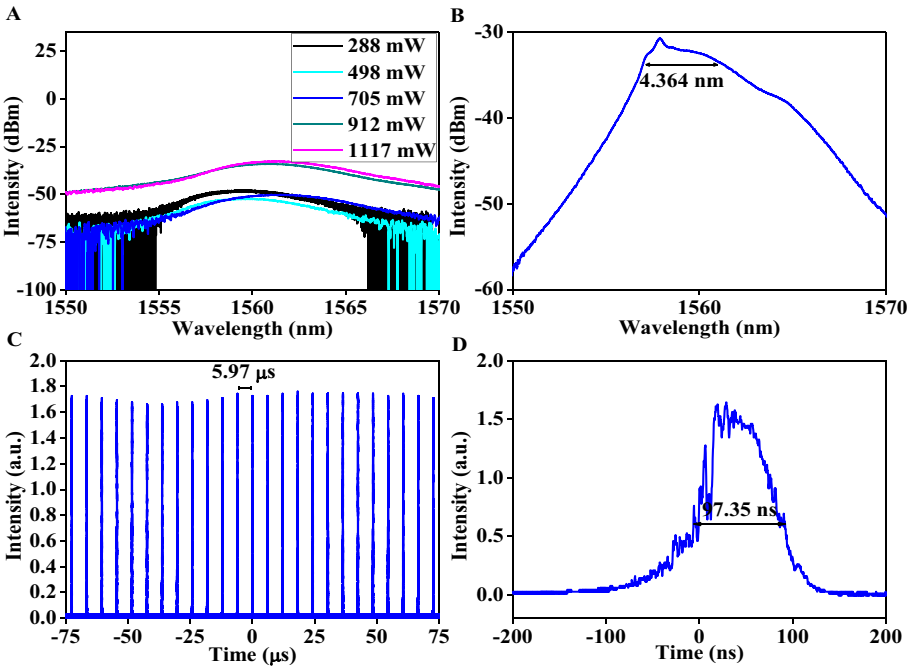

Fig. 3 **a** Corresponding optical spectra under the pump powers of 251 mW, 434 mW, 615 mW, 795 mW and 974 mW, respectively. **b** Optical spectrum under the pump power of 1152 mW. **c** Pulse train under the pump power of 1152 mW. **d** A single-pulse shape under the pump power of 1152 mW

1152 mW, the shape of the pulse evolves into non-rectangular structure. Figure 3b shows the corresponding optical spectrum under the pump power of 1152 mW. The central wavelength is 1557.878 nm and the 3 dB bandwidth is about 4.364 nm. It is different from that of square-wave pulse, indicating that the mode-locked operation is not square-wave pulse any more. The recorded pulse train is shown in Fig. 3c, the pulse interval is 5.97 μs, which also corresponding to the fundamental frequency of 167.62 kHz. Single-pulse shape shown in Fig. 3d also proves that the square-wave pulse is broken.

Because the original purpose of our experimental design is to obtain high-power and large-energy mode-locked pulse lasers, thus, in the experiment, we mainly adjust the pump power to the highest level available, and obtain different forms of mode-locked pulse output by adjusting the polarization controller.

First, under the maximum pump power of 2318 mW, by adjusting the PCs, a high-energy mode-locked operation with wide pulse width was obtained, its output performance is depicted in Fig. 4. The emission spectrum exhibits a central wavelength of 1558.415 nm and a 3 dB bandwidth of about 2.014 nm (Fig. 4a). Figure 4b shows the RF spectrum recorded under a resolution of 1 kHz, it is obvious that the central frequency is located at 167.62 kHz with a signal-to-noise ratio of ~ 50 dB, which fully proves that the mode-locked pulse exhibits high stability. The recorded pulse train is shown in Fig. 4c, the pulse interval is 5.97 μs, which also corresponds to the fundamental frequency of 167.62 kHz. A typical pulse shape was provided in Fig. 4d, the pulse width is about 509.15 ns. Additionally, the maximum average output power is tested to be about 128.98 mW, corresponding to a pulse energy of 769.48 nJ, and in comparison with previous works, the output performance, especially pulse energy, showed significant enhancement. To our knowledge, 769.48 nJ is the recorded output pulse energy obtained within a mode-locked Er-doped fiber laser oscillator. It should be pointed out that the pulse repetition rate does not increase or the pulse shape does not split under such a large pulse energy. The main reason is that the broadening of the pulse width balances the influence of peak power.

Meanwhile, under the maximum pump power of 2318 mW, the adjustment of the PCs also led to the formation of pulse splitting or higher-order soliton operations. The recorded information of the high-energy pulse splitting mode-locked operation are described in Fig. 5. Figure 5a shows a typical dual-wavelength optical spectrum. The central wavelengths and corresponding 3 dB bandwidths are 1556.315 and 1557.130 nm, and 0.322 and 0.336 nm, respectively. Figure 5b shows the RF spectrum located at the fundamental frequency of 167.62 kHz, which was recorded under a resolution of 1 kHz. The signal-to-noise ratio is about 24 dB, which shown an obvious degradation in comparison with the mentioned operations, which is mainly due to the effect of the pulse splitting (described in Fig. 5d). Because, the signal-to-noise ratio of the fundamental frequency was recorded based on the calculation of the pulse-to-pulse time of the recorded pulse train, the splitting of the pulses will lead to a large fluctuation and lead to the reduction of the contrast ratio. The recorded pulse train and single-pulse shape are shown in Fig. 5c, d. The pulse repetition rate also corresponds to the fundamental frequency of

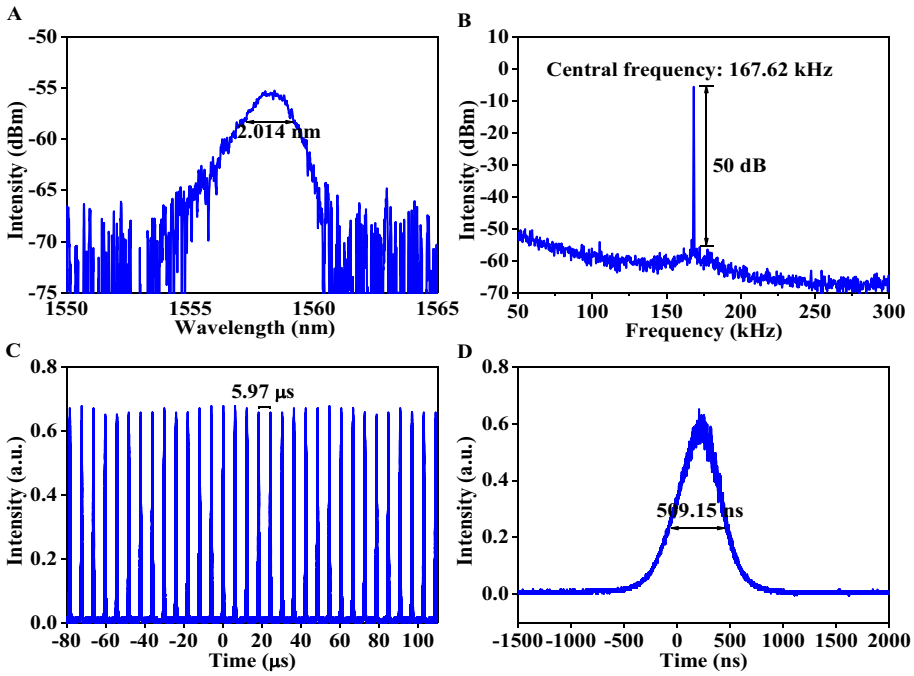

Fig. 4 Output characteristics of the large-energy mode-locked operation. **a** Optical spectrum. **b** Frequency spectrum. **c** Pulse train. **d** A typical single-pulse shape

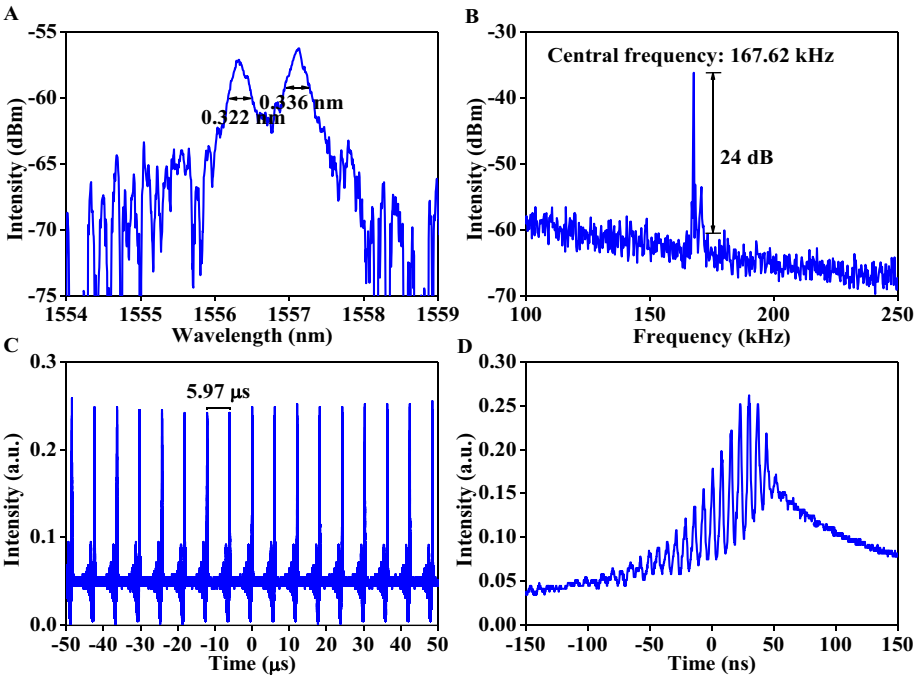

Fig. 5 Output of the pulse splitting mode-locked operation. **a** Optical spectrum. **b** Frequency spectrum. **c** Pulse train. **d** A typical single-pulse shape

167.62 kHz. Pulse splitting performance is fully presented in Fig. 5d. For the pulse splitting operation, the maximum average output power is 147.73 mW, corresponding to a pulse energy of 881.34 nJ. However, as is shown in Fig. 5d, the record pulses are actually an operation of pulse splitting, for this condition, the calculation of the pulse energy is not accurate as single-pulse regime. In comparison with the mentioned large-energy wide-pulse operation, the peak power limitation effect is decreased due to the splitting of the pulse instead of broadening of the pulse width.

Among the described large-energy and pulse splitting operations, for decreasing the influence of the high peak power and large energy, the mechanisms of broadening of the pulse and splitting of the pulse shape have been investigated. In addition, it is well known that increasing pulse repetition frequency can also reduce pulse energy, so as

to reduce the effect of various nonlinear optical progress caused by large pulse energy and high peak power.

In our experiment, under the maximum pump power of 2318 mW, by adjusting the PCs properly, harmonic order mode-locked operations including second and third order have also been recorded. Figure 6 shows the characteristics of the second-order harmonic mode-locked operation. The central wavelength and the 3 dB bandwidth of the emission spectrum (shown in Fig. 6a) are 1557.928 and 0.481 nm, respectively. Figure 6b shows the RF spectrum recorded under a resolution of 1 kHz. The central frequency located at 335.24 kHz with a signal-to-noise ratio of ~ 29 dB is recorded, indicating that the mode-locked operation is in the second-order mode-locked state. The corresponding pulse train with a pulse-to-pulse time of 2.99 μs is shown in Fig. 6c. A typical pulse shape with a pulse width of 12.42 ns is depicted in Fig. 6d. Obviously, no pulse splitting phenomenon is presented. Meanwhile, the maximum average output power is as high as 145.34 mW, corresponding to a pulse energy of 433.54 nJ, indicating that the pulse energy decreases due to the increase of the pulse repetition.

Besides the second-order harmonic mode-locked operation, third-order harmonic mode-locked operation can also be obtained. The emission spectrum with a central wavelength of 1557.908 nm and a 3 dB bandwidth of ~ 0.671 nm is shown in Fig. 7a. Figure 7b shows the RF spectrum recorded under a resolution of 1 kHz. The repetition rate is 497.85 kHz, corresponding to a 2.01 μs pulse interval (Fig. 7c), indicating that the mode-locked operation is belonging to a third order. Additionally, the signal-to-noise ratio is ~ 31 dB, indicating that the fundamental mode-locked laser is running stably. It is obvious that for the second- and third-order harmonic mode-locked operations, signal-to-noise ratios also decreased. In comparison with the pulse splitting operation, the reason for the decline of the signal-to-noise ratios is mainly due to the reduction of the single-pulse energy. The single-pulse shape with a pulse width of 12.59 ns is provided in Fig. 7d. At this time, the measured maximum average output power is as high as 142.05 mW and the single-pulse energy is 285.33 nJ.

Due to the fact that the pulse energies were calculated by the ratio of the average output power and the pulse repetition rate, however, for the mode-locked operations exhibiting the pulse splitting phenomenon, such as the mentioned square-wave pulse, the large-energy and the pulse splitting operations, the calculations of the pulse energies were not extremely accurate, meanwhile, for the harmonic mode-locked operations, the calculations were right due to the smooth single-pulse shapes. Besides, for all the mentioned mode-locked operations, the pulse widths of the mode-locked operations were all larger than that of traditional soliton operations. The reasons can be summarized as: first, the large dispersion value of $-26.6\ ps^2$ exhibited obvious dispersion effect on the formation of the mode-locked pulses, which will lead to the broadening of the pulse width. In addition, under high pump power, the effect of the high peak power should not be ignored, the peak-power limitation effect also leads to a wide pulse width.

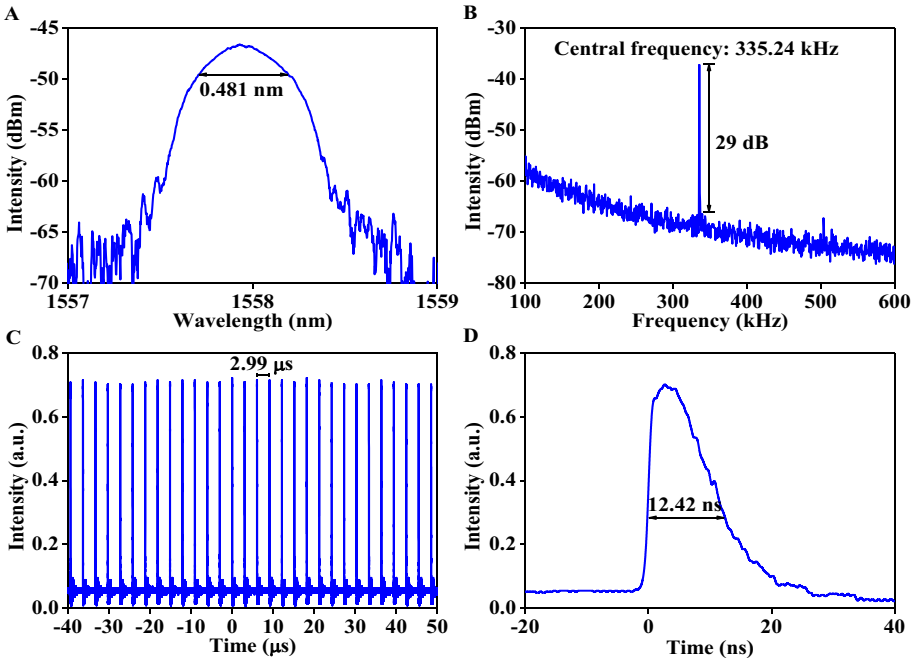

Fig. 6 Characteristics of the second-order harmonic mode-locked operation. **a** Optical spectrum. **b** Frequency spectrum. **c** Pulse train. **d** A typical single-pulse shape

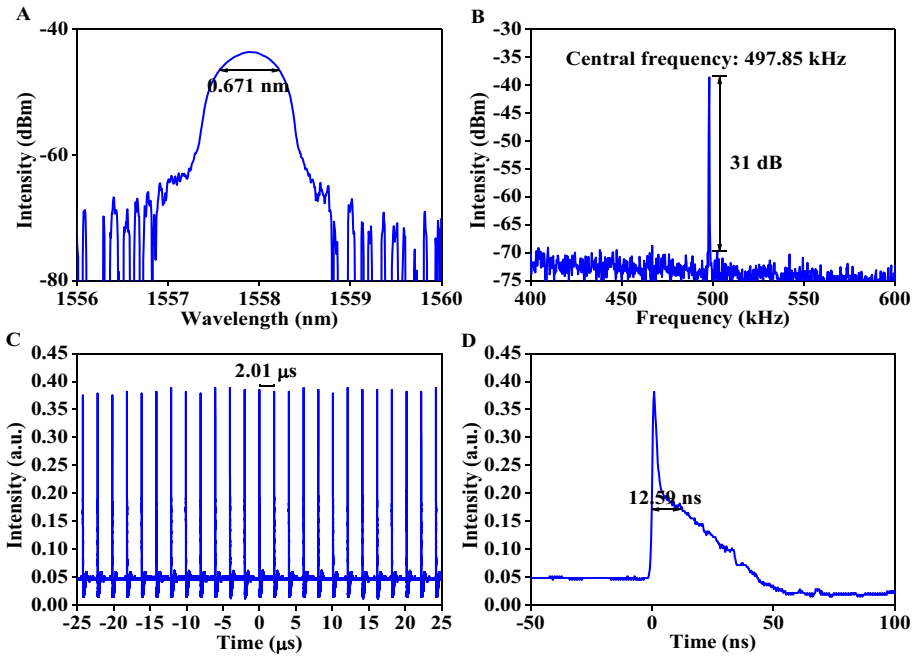

Fig. 7 Characteristics of the third-order harmonic mode-locked operation. **a** Optical spectrum. **b** Frequency spectrum. **c** Pulse train. **d** A typical single-pulse shape

4 Conclusion

In conclusion, first, large-energy square-wave soliton pulses within a passively mode-locked Er-doped fiber laser were generated. In addition, under the maximum pump power of 2318 mW, several kinds of large-energy mode-locked operations were also demonstrated. The maximum pulse energy was as high as 881.34 nJ, which exhibited significant enhancement in comparison with previous works. To our knowledge, 881.34 nJ is the maximum pulse energy obtained within Er-doped mode-locked fiber lasers so far. Especially, experimental phenomena including broadening of the pulse width, splitting of the pulse shape and increase of the pulse repetition rate for decreasing the influence of the high peak power and large energy were investigated systematically. Our experiment result fully presents the advantages of our design and provide meaningful reference for investigating the high-power and large-energy mode-locked Er-doped oscillators.

Acknowledgements This work was supported in part by the National Natural Science Foundation of China (Grant Nos. 61971271, 11904213, 11747149), Shandong Province Natural Science Foundation (ZR2018QF006), the Taishan Scholars Project of Shandong Province (Tsqn20161023), Primary Research and Development Plan of Shandong Province (2018GGX101018) and supported by "Opening Foundation of Shandong Provincial Key Laboratory of Laser Technology and Application".

References

1. K.D. Niu, R.Y. Sun, Q.Y. Chen, B.Y. Man, H.N. Zhang, Passively mode-locked Er-doped fiber laser based on SnS_2 nanosheets as a saturable absorber. Photonics Res. **6**(2), 72–76 (2018)
2. P.G. Yan, A.J. Liu, Y.S. Chen, J.Z. Wang, S.C. Ruan, H. Chen, J.F. Ding, Passively mode-locked fiber laser by a cell-type WS_2 nanosheets saturable absorber. Sci. Rep. **5**(1), 12587 (2015)
3. N. Ming, S.N. Tao, W.Q. Yang, Q.Y. Chen, R.Y. Sun, C. Wang, S.Y. Wang, B.Y. Man, H.N. Zhang, Mode-locked Er-doped fiber laser based on PbS/CdS core/shell quantum dots as saturable absorber. Opt. Express **26**(7), 9017–9026 (2018)
4. R.I. Woodward, E.J.R. Kelleher, Towards 'smart lasers': self-optimisation of an ultrafast pulse source using a genetic algorithm. Sci. Rep. **6**(1), 37616 (2016)
5. L.G. Guo, X.X. Shang, R. Zhao, H.N. Zhang, D.W. Li, Nonlinear optical properties of ferromagnetic insulator $Cr_2Ge_2Te_6$ and its application for demonstrating pulsed fiber laser. Appl. Phys. Express **12**(8),082006 (2019)
6. F.Y. Zhao, Y.S. Wang, H.S. Wang, Z.J. Yan, X.H. Hu, W. Zhang, T. Zhang, K.M. Zhou, Ultrafast soliton and stretched-pulse switchable mode-locked fiber laser with hybrid structure of multimode fiber based saturable absorber. Sci. Rep. **8**(1), 16369 (2018)
7. T.H. Liu, D.F. Jia, Y. Liu, Z.Y. Wang, T.X. Yang, Generation of microseconds-duration square pulses in a passively mode-locked fiber laser. Opt. Commun. **356**, 416–420 (2015)
8. N.N. Xu, N. Ming, X.L. Han, B.Y. Man, H.N. Zhang, Large-energy passively Q-switched Er-doped fiber laser based on CVD-Bi_2Se_3 as saturable absorber. Opt. Mater. Express **9**(2), 373–383 (2019)

9. X.X. Shang, L.G. Guo, J.J. Gao, S.Z. Jiang, X.L. Han, Q.X. Guo, X.H. Chen, D.W. Li, H.N. Zhang, 170 mW-level mode-locked Er-doped fiber laser oscillator based on nonlinear polarization rotation. Appl. Phys. B **125**(10), 193 (2019)
10. D.P. Zhou, L. Wei, B. Dong, W.K. Liu, Tunable passively Q-switched erbium-doped fiber laser with carbon nanotubes as a saturable absorber. IEEE Photonics Technol. Lett. **22**(1), 9–11 (2010)
11. Q.X. Guo, J. Pan, Y.J. Liu, H.P. Si, Z.Y. Lu, X.L. Han, J.J. Gao, Z.T. Zuo, H.N. Zhang, S.Z. Jiang, Output energy enhancement in a mode-locked Er-doped fiber laser using CVD-Bi_2Se_3 as a saturable absorber. Opt. Express **27**(17), 24670–24681 (2019)
12. D.J. Richardson, R.I. Laming, D.N. Payne, V. Matsas, M.W. Phillips, Selfstarting, passively mode-locked erbium fiber ring laser based on the amplifying Sagnac swith. Electron. Lett. **27**(6), 542–544 (1991)
13. H.A. Haus, K. Tamura, L.E. Nelson, E.P. Ippen, Stretched-pulse additive pulse mode-locking in fiber ring lasers: theory and experiment. IEEE J. Quantum Electron. **31**(3), 591–598 (1995)
14. F.Ö. Ilday, J.R. Buckley, W.G. Clark, F.W. Wise, Self-similar evolution of parabolic pulses in a laser. Phys. Rev. Lett. **92**, 213902 (2004)
15. B. Oktem, C. Ülgüdür, F.Ö. Ilday, Soliton–similariton fibre laser. Nat. Photon. **4**, 307–311 (2010)
16. S. Kobtsev, S. Kukarin, S. Smirnov, A. Latkin, Generation of double-scale femto/pico-second optical lumps in mode-locked fiber lasers. Opt. Express **17**(23), 20707–20713 (2009)
17. S. Kobtsev, S. Kukarin, Y. Fedotov, Ultra-low repetition rate mode-locked fiber laser with high-energy pulses. Opt. Express **16**(26), 21936–21941 (2008)
18. X.M. Zhang, C. Gu, G.L. Chen, B. Sun, L.X. Xu, A.T. Wang, H. Ming, Square-wave pulse with ultra-wide tuning range in a passively mode-locked fiber laser. Opt. Lett. **37**(8), 1334–1336 (2012)
19. X. Li, X. Liu, X. Hu, L. Wang, H. Lu, Y. Wang, W. Zhao, Long-cavity passively mode-locked fiber ring laser with high-energy rectangular-shape pulses in anomalous dispersion regime. Opt. Lett. **35**(19), 3249–3251 (2010)
20. X.M. Liu, D. Mao, Compact all-fiber high-energy fiber laser with sub-300-fs duration. Opt. Express **18**(9), 8847–8852 (2010)
21. C.M. Ouyang, P.P. Shum, K. Wu, J.H. Wong, X. Wu, H.Q. Lam, S. Aditya, Dissipative soliton (12 nJ) from an all-fiber passively mode-locked laser with large normal dispersion. IEEE Photonics J. **3**(5), 881–887 (2011)
22. D. Mao, X.M. Liu, L.R. Wang, H. Lu, H. Feng, Generation and amplification of high-energy nanosecond pulses in a compact all-fiber laser. Opt. Express **18**(22), 23024–23029 (2010)
23. N.B. Chichkov, K. Hausmann, D. Wandt, U. Morgner, J. Neumann, D. Kracht, High-power dissipative solitons from an all-normal dispersion erbium fiber oscillator. Opt. Lett. **35**(16), 2807–2809 (2010)
24. K. Jiang, C.M. Ouyang, P.P. Shum, K. Wu, J.H. Wong, High-energy dissipative soliton with MHz repetition rate from an all-fiber passively mode-locked laser. Opt. Commun. **285**(9), 2422–2425 (2012)
25. S.K. Wang, Q.Y. Ning, A.P. Luo, Z.B. Lin, Z.C. Luo, W.C. Xu, Dissipative soliton resonance in a passively mode-locked figure-eight fiber laser. Opt. Express **21**(2), 2402–2407 (2013)
26. G. Semaan, F.B. Braham, J. Fourmont, M. Salhi, F. Bahloul, F. Sanchez, 10 μJ dissipative soliton resonance square pulse in a dual amplifier figure-of-eight double-clad Er: Yb mode-locked fiber laser. Opt. Lett. **41**(20), 4767–4770 (2016)
27. F.B. Braham, G. Semaan, F. Bahloul, M. Salhi, F. Sanchez, Experimental optimization of dissipative soliton resonance square pulses in all anomalous passively mode-locked fiber laser. J. Opt. **19**, 105501 (2017)
28. M. Salhi, G. Semaan, F. Ben Braham, J. Fourmont, F. Bahloul, F. Sanchez, Route to high-energy dissipative soliton resonance pulse in a dual amplifier figure-of-eight fiber laser. Proc. SPIE **10228**, 102280 (2017)
29. K. Krzempek, K. Abramski, Dissipative soliton resonance mode-locked double clad Er: Yb laser at different values of anomalous dispersion. Opt. Express **24**(20), 22379–22386 (2016)
30. X.L. Tian, M. Tang, P.P. Shum, Y.D. Gong, C. Lin, S.N. Fu, T.S. Zhang, High-energy laser pulse with a submegahertz repetition rate from a passively mode-locked fiber laser. Opt. Lett. **34**(9), 1432–1434 (2009)
31. N.N. Xu, H.N. Zhang, B.Y. Man, Various large-energy soliton operations within an Er-doped fiber laser with bismuth selenide as a saturable absorber. Appl. Opt. **57**(30), 8811–8818 (2018)